

Computer analysis of rarefied aerodynamics around a winged space-plane for Mars entry

Gennaro Zuppardi*¹ and Giuseppe Mongelluzzo^{1,2a}

¹Department of Industrial Engineering – Aerospace Division,
University of Naples “Federico II”, Piazzale Tecchio 80, 80125 Naples, Italy

²INAF – Osservatorio Astronomico di Capodimonte, Salita Moiariello, 16, 80131, Naples, Italy

(Received February 12, 2021, Revised April 7, 2021, Accepted May 18, 2021)

Abstract. The forthcoming use of Orion for Mars landing stimulated Zuppardi to compute global aerodynamic coefficients in rarefied flow along an entry path. Zuppardi and Mongelluzzo also studied Aerodynamics of a blunt cylinder, provided with flapped fins, as a possible alternative to Orion for Mars Entry, Descent and Landing. Computer tests were carried out, in the altitude interval 60-100 km, by three codes: i) home made code computing the entry trajectory, ii) Direct Simulation Monte Carlo code (DS2V), solving 2D/axisymmetric flow field and computing local quantities, iii) Direct Simulation Monte Carlo code (DS3V) solving 3D flow field and computing global aerodynamic coefficients. The comparison of the aerodynamic behaviour of the two capsules in axisymmetric flow field verified that heat flux and wall temperature for the finned-cylinder are higher than those of Orion. The DS3V results verified that Orion is better than the finned-cylinder to produce an aerodynamic force for slowing down the capsule. On the contrary, the results indicated that the finned-cylinder is better in terms of attitude control capability. The purpose of the present paper is to compare Aerodynamics of: Orion, finned-cylinder, a hypothetical, winged space-plane in high altitude Mars entry path. Computations were carried out by means of the two above mentioned DSMC codes, along both orbit and direct entry trajectories. While the global aerodynamic coefficients of the space-plane are comparable with those of the finned cylinder, the aerodynamic and thermal stresses (or pressure, temperature and heat flux) at the nose stagnation point are higher for the space-plane. Therefore, the finned-cylinder seems to be a valid alternative to Orion.

Keywords: Mars space-plane; Orion capsule; finned-cylinder capsule; entry trajectory; direct simulation Monte Carlo method

1. Introduction

Orion is a manned, partially reusable capsule for future space exploration. It was conceived as a rescue shuttle for the International Space Station (ISS). NASA originally started this project to replace the retired Space Shuttle as a link to/from ISS (Moss *et al.* 2006). According to the NASA's Artemis program (2021), Orion will be used to transport instruments and astronauts in new manned lunar missions as well as in landing on Mars.

NASA is currently still developing this project. The first, unmanned flight test took place on

*Corresponding author, Lecturer, E-mail: zuppardi@unina.it

^aPh.D., E-mail: giuseppe.mongelluzzo@unina.it

Dec. 5, 2014. Orion was launched from Cape Canaveral, reached an altitude of 5700 km, made two terrestrial orbits and finally splashed down into Pacific Ocean off the coast of California. Aerodynamics of Orion in Earth atmosphere entry from ISS was already studied by Moss *et al.* (2006) in all hypersonic rarefaction regimes i.e., from free molecular flow to continuum. Zuppardi (2020) computed the global aerodynamic coefficients along a Mars direct entry path at high altitudes and performed a sensitivity analysis of the longitudinal moment and equilibrium angle of attack in terms of position of the center of gravity. Zuppardi and Mongelluzzo (2021a, b) also studied Aerodynamics of a blunt cylinder, provided with flapped fins, as a possible alternative to Orion for Mars Entry, Descent and Landing (EDL). Computations were carried out at high altitude by a home-made code (Zuppardi and Savino 2015) for the computation of the entry trajectory and by two Direct Simulation Monte Carlo (DSMC) codes: DS2V (Bird 2008), solving 2D/axisymmetric flow field in the altitude interval 60-100 km, DS3V (Bird 2006a), solving 3D flow field at the altitudes of 80, 90 and 100 km in the interval of angles of attack 0-40 deg. The comparison of the aerodynamic behaviour of the two capsules verified that, being the curvature radius of the cylinder smaller than the curvature radius of the Orion shield, heat flux and wall temperature are higher than those of Orion. The DS3V results verified that Orion is better than the finned-cylinder to produce an aerodynamic force at low angles of attack for slowing down the capsule. On the contrary, the results indicated that the finned-cylinder is better in terms of attitude control capability; the finned-cylinder is in stable equilibrium at zero angle of attack. Certainly, geometries of fins and flaps have to be optimized to increase the aerodynamic capabilities.

The interest of the aerospace scientific community for re-entering/entering capsules, provided with aerodynamic control surfaces, is not recent and is increasing. The Intermediate Experimental Vehicle (IXV, Roncioni *et al.* 2007, 2011a, b) is an interesting example of such a capsule; IXV is provided of two large body flaps making possible an aerodynamic control of its attitude along a re-entry path in Earth atmosphere.

The aim of the present paper is to compare Aerodynamics of both Orion and finned-cylinder with that of a hypothetical, winged space-plane in high altitude Mars entry path. A “classic” winged space-plane for Mars EDL similar to the American Space Shuttle or to the Russian Buran has been not yet designed; a limitation to the development of such a project is due also to the lack of landing runways on Mars. Thus it can be seen as a branch of space research to be potentially investigated in the future.

For the purpose of this paper which, for what said before, is purely speculative, a winged space-plane very similar to the Italian Flight Test Bed (FTB_2, Curreri *et al.* 2003), devoted at studying re-entry to Earth, has been here considered. Dimensions of the tested space-plane are comparable with those of Orion and of the finned-cylinder. Since Aerodynamics of a lifting body is much more complex than that of a non-lifting body like a sphere-cone capsule, for the sake of completeness, computation of velocity was carried out along both an orbit trajectory and a direct entry trajectory. The effects of the very different geometries of the three bodies on the flow field were also evaluated.

2. Direct simulation Monte Carlo method and DS2V/DS3V codes

The DSMC method (Bird 1998, Shen 2005, Bird 2013) is a stochastic method, solving the flow fields in transitional regime i.e. from continuum low density regime to free molecule regime. As well known, the DSMC method is an indispensable tool for solving rarefied flow fields because of the failure of the Navier-Stokes equations due to the failure of the Chapman-Enskog theory for the

computation of transport coefficients. On the other hand, the solution of the Boltzmann equation is very difficult. Furthermore, the Boltzmann equation can not consider chemical reactions; these are very important in highly energized flows like those met along an entry path. Even though the DSMC method is a mature tool, widely accepted by the scientific community, however here it will be shortly recalled in order to define the parameters defining the quality of the calculations and therefore the reliability of the results.

The DSMC method relies on the kinetic theory of gases and considers gas as made up of millions of simulated molecules, each one representing a large number of real molecules in the physical space. For example, in the present computations, each simulated molecule represented $10^{12} \div 10^{13}$ and $10^6 \div 10^8$ real molecules for the 3D and 2D/axisymmetric computations, respectively.

The evolution of the molecules in terms of velocity, spatial coordinates, thermodynamic and chemical status is produced by molecule-molecule collisions and molecule-surface interactions within the simulated physical space. This is divided into cells both for selecting the colliding molecules and for sampling the thermo-fluid-dynamic quantities. The molecules in a cell represent those at the same location in the physical field. The method does not rely on integration of differential equations therefore it does not suffer from numerical instabilities but it is inherently unsteady with a steady solution achievable after a sufficiently long simulation time.

The basic assumption of the method is the temporal decoupling of motion and collision of the simulated molecules. In the motion phase, the simulated molecules move ballistically at their own velocity over the global time step. Molecules change position in the flow field and interact with the surface of the body under study. In the collision phase, a couple of colliding molecules are selected in the cell. Chemical reactions take place, both colliding molecules exchange energy among the translational and the interior degrees of freedom (rotation, vibration), thus their velocity changes. The gas macroscopic properties (density, temperature, etc.) and surface macroscopic properties (pressure, shear stress, heat flux, etc.) are computed by sampling and then by averaging, in each cell and on each elemental area of the body surface, molecular quantities (number of molecules, gas composition, momentum, kinetic energy, internal energy, etc.) every 20-30 global time steps.

Both DS2V and DS3V are “sophisticated”; in literature, a sophisticated code is labeled also as DSMC07. A DSMC07 code implements computing procedures achieving both greater efficiency and accuracy with respect to a “basic” DSMC code (Bird 2006b, Bird *et al.* 2009, Gallis *et al.* 2009). In literature, a basic code is labeled also as DSMC94.

A DSMC07 code is self-diagnosing; it provides the user with indication about the quality of the computations and therefore about the reliability of the results. The adequacy of the number of simulated molecules and of cells and therefore the quality of the results is quantified by the ratio of the mean collision separation (mcs) or the distance between the collision partners and the mean molecular free path (λ): mcs/λ . According to Bird (2006b), this ratio has to be less than unity for a good quality of results and less than 0.2 for an optimal quality of results. DS2V provides in output the value of mcs/λ averaged over the computational domain. DS3V provides in output only the maximum value. Thus the average values that will be shown next have been deduced graphically.

Furthermore, DS2/3V provide indication about the stabilization of a computation. Stabilization is achieved when the profile of the number of simulated molecules, as a function of the simulated time, becomes jagged and included within a band which defines the standard deviation of the number of simulated molecules. In a DSMC computation, increasing t_s is beneficial because the longer the simulation time the larger the number of samples of the molecular quantities for the computation of the macroscopic fluid-dynamic quantities. Furthermore, increasing the number of

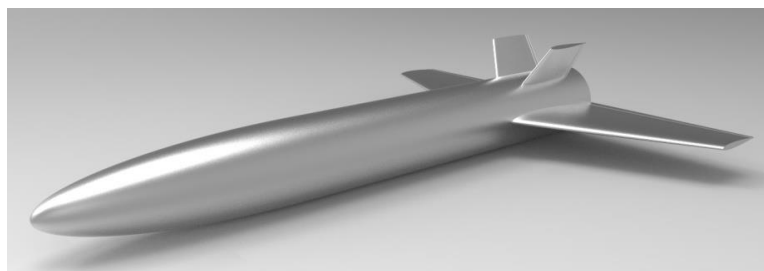
samples is equivalent to a calculation with a larger number of simulated molecules, making possible the fluctuations match those in the real gas.

3. Space-plane geometry

Fig. 1(a) shows a rendering of the tested space-plane that, as already said, is very similar in shape and in dimensions to the Italian Flight Test Bed (FTB_2, Currei *et al.* 2003). Table in figure reports the most meaningful quantities. The platform surface and the overall length have been used for scaling aerodynamic force and moment to the related coefficients. The length of the space-plane is equal to those of the finned-cylinder and of Orion. The center of gravity (CG) was considered to be located on the axis ($y_{cg}=0.0$ m, $z_{cg}=0.0$ m) and at $x_{cg}=3.0$ m from the nose tip.

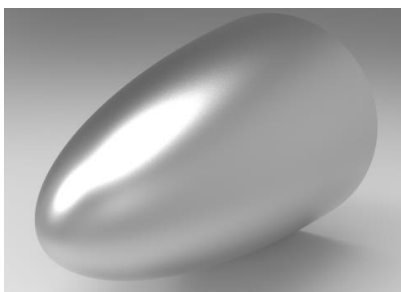
The reflection of molecules from the body surface was considered diffusive fully accommodated. Wall temperature was constant along the whole surface of vehicle ($T_w=300$ K). Since computations were carried out only in symmetric flight, it was possible to consider for the 3D computations only half body. RHINOCEROS[®] approximated the half-surface into 25830 triangles. The computation dominion was a parallelepiped: $X=4.7$ m, $Y=2$ m, $Z=1.8$ m.

Computations of local quantities as per heat flux, pressure and temperature, has been carried out on the nose which, as well known, is the most stressed part of a space-plane. The space-plane nose was considered to be the first 0.5 m of the fuselage (Fig.1(b)). Computations were carried out at zero angle of attack by means of the DS2V code. Indeed, the routine, built in DS2V for drawing the body geometry, makes possible a more precise definition of the stagnation point compared with that produced by RHINOCEROS. The computational domain was a rectangle in the meridian plane: $X=0.7$ m, $Y=0.25$ m. The nose surface was approximated into 100 intervals, more dense around the stagnation point.



Platform surface [m ²]	3.47
Overall length (L) [m]	4.0
Root chord [m]	0.9
Tip chord [m]	0.4
Wing span [m]	3.0
Wing surface [m ²]	1.63
Aileron surface [m ²]	0.14
Mass [kg]	3155

(a)



Length (L_N) [m]	0.5
Base diameter [m]	0.188
Nose radius [m]	0.042

(b)

Fig. 1 Rendering of the space-plane (a) and rendering of the space-plane nose (b)

Table 1 Input data to DS2V/3V and free stream density, Knudsen number

h [km]	T _∞ [K]	N _∞ [1/m ³]	ρ _∞ [kg/m ³]	Kn _{∞L}
100	126.9	8.22×10 ¹⁷	5.88×10 ⁻⁸	2.24×10 ⁻¹
90	125.5	3.73×10 ¹⁸	2.67×10 ⁻⁷	4.94×10 ⁻²
80	135.4	1.98×10 ¹⁹	1.42×10 ⁻⁶	9.33×10 ⁻³
70	146.2	8.26×10 ¹⁹	5.92×10 ⁻⁶	2.23×10 ⁻³
60	142.7	3.26×10 ²⁰	2.34×10 ⁻⁵	5.65×10 ⁻⁴

4. Mars atmosphere

Mars atmosphere is made of 7 chemical species O₂, N₂, NO, CO, CO₂, C, A_r and its composition is constant with altitude. The mole fractions, used in the present computations, are 0.00176, 0.04173, 0.00014, 0.00108, 0.93399, 0.00396, 0.01734, respectively. Due to dissociation along an entry path, the presence of atomic oxygen and atomic nitrogen was considered. Therefore, in these simulations, the working gas is a mixture of 9 chemical species. The chemical model, proposed by Bird in Ver. 3.3 of the DS2V code (Bird 2005) has been implemented also in the current versions of DS2V (4.5) and DS3V (2.6). This model is made of 54 reactions: 40 dissociations, 7 forward (or endothermic) exchanges, 7 reverse (or exothermic) exchanges.

The Mars Global Reference Atmospheric Model (GRAM-2001, Justus and Johnson 2001) provided the atmosphere parameters (temperature, density therefore number density). The parameters used in the present computations are those reported by Justus and Johnson in the altitude interval -1.365÷194.654 km with a step of about 5 km. Here, the parameters at the intermediate altitudes in each step, used for the computation of the entry trajectory, were computed by linear interpolation. Since the ambient quantities have to be interpreted as free stream quantities, they will be labeled by the subscript ∞.

Computations have been carried out in the altitude interval between 60 and 100 km. Table 1 reports input data to DS2/3V codes (temperature T_∞, number density N_∞) and some fluid-dynamic parameters (density ρ_∞, and Knudsen number (Kn_{∞L}, based on the space-plane length). The flow field can be considered in transitional regime. According to Moss (1995) the transitional regime is defined in terms of the global Knudsen number by: 10⁻³<Kn_{∞L}<50.

5. Test conditions

The entry trajectories of the space-plane were computed by integration of the equations of dynamics (Eqs.1(a) and 1(b)) of the space-plane (Zuppari and Savino 2015). Since the explicit presence of the lift in Eq.1(b) causes instability in the integration process, lift has been merged with the drag to form the resulting global aerodynamic force F and the corresponding coefficient C_F (C_F = √(C_L² + C_D²)). Therefore, in the present calculations, the ballistic parameter is defined as m/S/C_F instead of m/S/C_D:

$$\frac{dV}{dh} = \frac{1}{2} \frac{\rho V}{\sin \gamma} \frac{SC_F}{m} - \frac{g}{V} \quad (1a)$$

$$\frac{d\gamma}{dh} = \frac{1}{R \sin \gamma} - \frac{g}{V^2} \frac{1}{\operatorname{tg} \gamma} \quad (1b)$$

being: V the velocity, γ the flight path angle, g the gravity acceleration, R the curvature radius of the trajectory, m the capsule mass.

Eq. 1(a) and 1(b) were integrated numerically by a forward scheme with a first order approximation (Euler method). Integration started from $h=100$ km, the step was 0.02 km. As said before, computations were carried out considering both a direct and an orbital entry trajectory. The initial data of integration procedure for both trajectories are reported in Table 2. Velocity and angle of entry are those of Pathfinder for the calculation of the direct re-entry trajectory and of Viking 1/2 for the calculation of the orbital re-entry trajectory (Braun and Manning 2006), respectively. For the two types of entry, three trajectories were considered, each one corresponding to a value of C_D , constant along the trajectories. As reported by Curreri *et al.* (2003), the aerodynamic efficiency of FTB_2 in transonic and hypersonic flow is 2.5 therefore the corresponding values of C_L were computed by $2.5 \cdot C_D$. Table 3 reports the values of C_D , C_L and C_F .

Fig. 2(a), 2(b) and 2(c) show the profiles of free stream velocity (V_∞), Mach number (Ma_∞) and Reynolds number ($Re_{\infty L}$) as functions of altitude. Velocity, input to DS2/3V codes and the corresponding Mach and Reynolds numbers are reported in Table 4 for the entry trajectories computed with $C_D=1$. Velocity and Mach number do not change meaningfully in the altitude

Table 2 Operative parameters at $h=100$ km for direct and orbit trajectories

Entry trajectory	Direct	Orbit
Entry velocity [m/s]	7260	4700
Entry Path Angle [deg]	14.06	17.00
Entry mass [kg]	8500	8500
Entry ballistic parameter [kg/m^2]	214	214
Entry angle of attack [deg]	0	0

Table 3 Drag, lift and aerodynamic force coefficients

C_D	C_L	C_F
0.50	1.25	1.15
1.00	2.50	2.69
1.50	3.75	4.04

Table 4 Free stream velocity, Mach and Reynolds numbers for direct and orbit entry: $C_D=1$

h [km]	Direct Entry			Orbit Entry		
	V_∞ [m/s]	Ma_∞	$Re_{\infty L}$	V_∞ [m/s]	Ma_∞	$Re_{\infty L}$
100	7260	39.3	2.46×10^2	4700	25.4	1.59×10^2
90	7265	39.5	1.13×10^3	4708	25.6	7.31×10^2
80	7269	38.1	5.58×10^3	4715	24.7	3.62×10^3
70	7273	36.7	2.17×10^4	4722	23.8	1.41×10^4
60	7271	37.1	8.78×10^4	4726	24.1	5.71×10^4

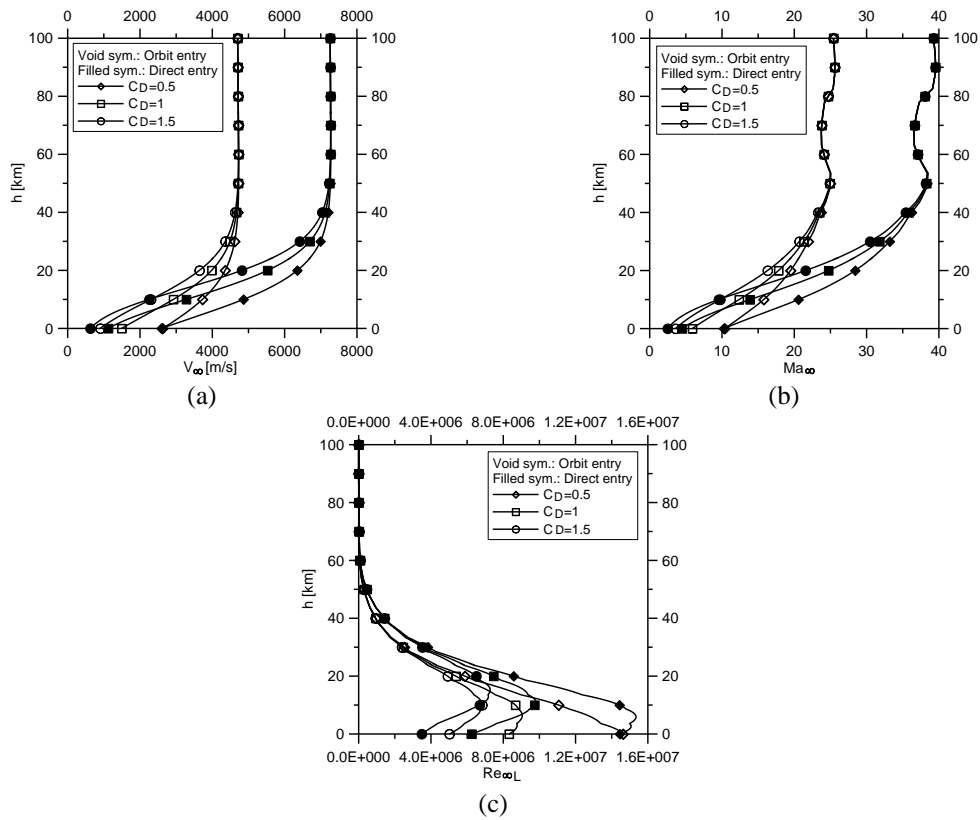


Fig. 2 Profiles of velocity (a), Mach number (b) and Reynolds number (c) as functions of altitude

interval 40-100 km. On the opposite, Reynolds number reduces by almost three orders of magnitude.

In order to evaluate thermal and mechanical stresses, or heat flux, wall temperature and pressure at the space-plane stagnation point, two sets of simulations were carried out at each altitude: i) non catalytic surface, ii) insulated surface. For the second case, DS2V considers the surface with zero thermal conductivity and takes into account, in the thermal balance, also the thermal radiation from the surface; the surface emissivity (ϵ) is required in input for each elemental area. In the present computations, the realistic value of $\epsilon=0.8$, constant along the space-plane surface, was used.

6. Quality of the results

Table 5 verifies the quality of the DS3V and DS2V results at the most severe conditions of: $h=80$ km and $\alpha=40$ deg for the 3D computations, $h=60$ km for the axisymmetric computations, respectively. N_M is the number of simulated molecules. Even though the Bird's criterion for an optimal quality of a DSMC computation ($mcs/\lambda \leq 0.2$, Bird 2006b) is not satisfied for the DS3V computations, however the values of mcs/λ , averaged on the flow field, are less than unity. The

Table 5 Quality of computations of DS3V and DS2V

Entry trajectory	DS3V: h=80 km, $\alpha=40$ deg			DS2V, h=60 km, $\alpha=0$ deg		
	N_M	mcs/ λ	t_s/t_f	N_M	mcs/ λ	t_s/t_f
Direct	9.15×10^5	0.5	107	2.25×10^7	0.015	3.49
Orbit	8.60×10^5	0.5	157	2.10×10^7	0.017	3.62

Bird's criterion is fully satisfied for the axisymmetric computations. A steady state condition is also achieved for both computations. In fact, as said before, for each computation, the profile of the number of the simulated molecules got jagged. Furthermore, as well known, a rule of thumb suggests considering an unsteady, fluid-dynamic computation stabilized when the ratio t_s/t_f is reasonably greater than unity, being t_s the simulation time and t_f the fluid-dynamic time, computed as the time necessary for the fluid to cross the length of the body under study ($L=4$ and $L_N=0.5$ m) at the free stream velocity: $t_f=L/V_\infty$ or $t_f=L_N/V_\infty$.

7. Analysis of the results

Figs. 3(a) and 3(b) verify that the influence of entry trajectories, at the three altitudes, is negligible for the global aerodynamic coefficients of interest for entry study, i.e. the resultant aerodynamic force (C_F) and the pitching moment coefficients (C_{MzTip} , the moment reduction pole is the nose tip). Certainly, the variation of high Mach numbers (see Table 4) does not produce meaningful effects on the aerodynamic coefficients (Mach number independence principle, Anderson 1998). Table 6 verifies that the percentage variations of C_F and C_{MzTip} between the values computed along the orbit entry and those calculated along the direct entry at the three altitudes and at $\alpha=40$ deg are negligible.

Figs.4(a)-4(e) show the comparison of the aerodynamic behavior of Orion, finned-cylinder and

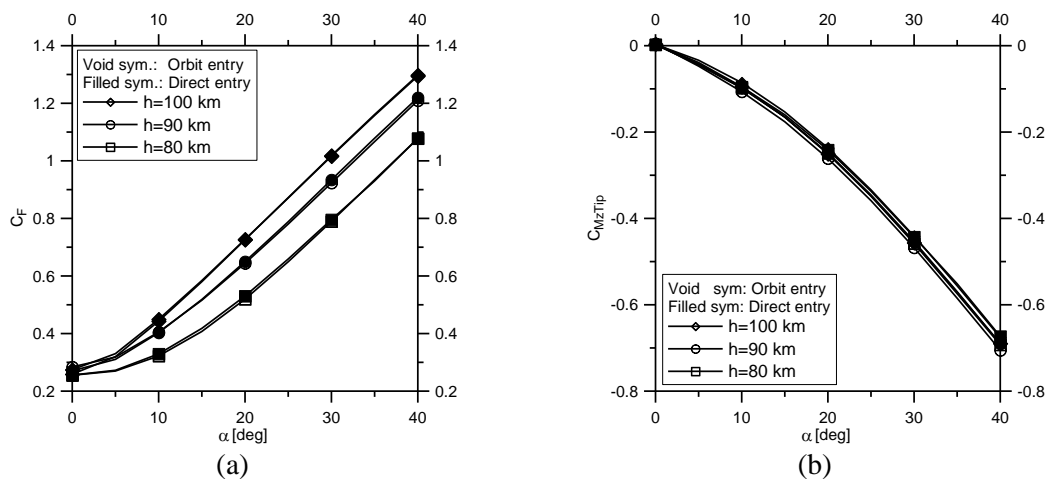


Fig. 3 Profiles of the space-plane resultant aerodynamic force (a) and pitching moment coefficients (b) as functions of the angle of attack

Table 6 Relative variations of aerodynamic coefficients: $\alpha=40$ deg

h [km]	$\Delta C_F / C_F$ %	$\Delta C_{MzTip} / C_{MzTip}$ %
100	-0.25	2.1
90	-0.86	2.2
80	-0.03	2.9

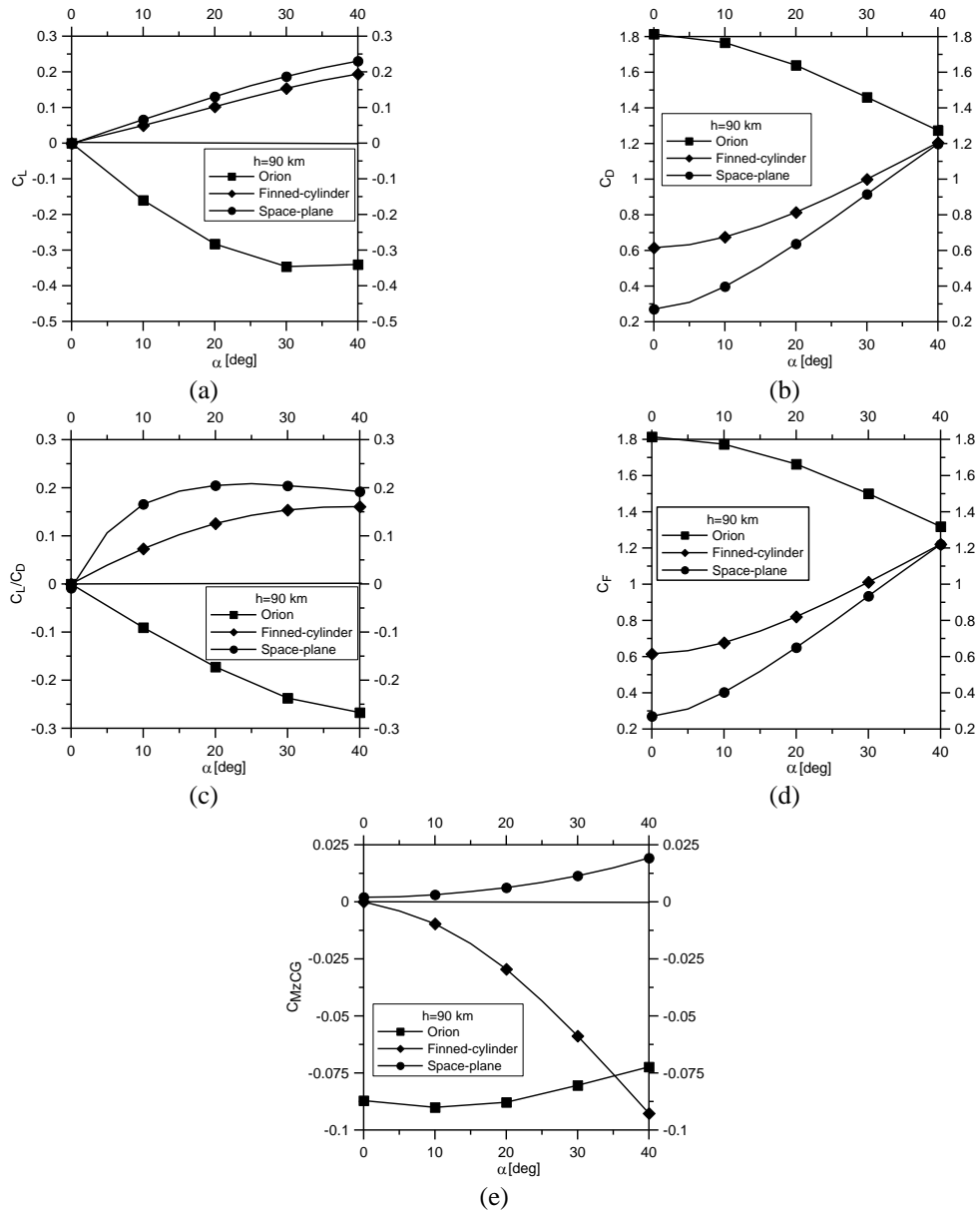


Fig. 4 Profiles of lift (a) and drag (b) coefficients, aerodynamic efficiency (c), resultant aerodynamic force (d) and pitching moment (e) coefficients as functions of angle of attack: $h=90$ km

Table 7 Stability derivatives $(dC_{MzCG}/d\alpha)_{\alpha=0}$

h [km]	Space-plane	Finned-cylinder
100	8.0×10^{-5}	-1.7×10^{-3}
90	1.1×10^{-4}	-9.6×10^{-4}
80	2.8×10^{-4}	4.0×10^{-5}

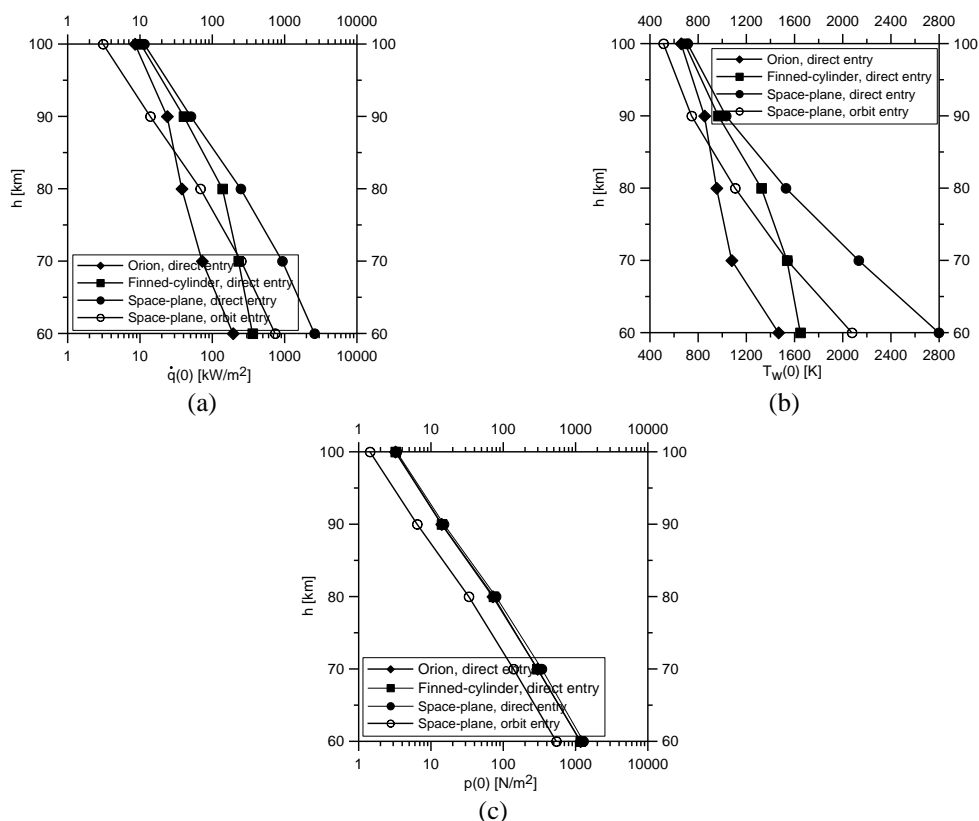


Fig. 5 Profiles of heat flux (a), surface temperature (b) and pressure (c) at the stagnation point as functions of altitude

space-plane, for example at $h=90$ km. Similar plots are obtained also at other altitudes. The profiles of the global aerodynamic coefficients of the finned cylinder and of the space-plane, apart those of the pitching moment (the reduction pole is the Center of Gravity), are similar. Orion does not get an equilibrium condition in the interval of angles of attack 0-40 deg.

It seems that the aerodynamic behavior of the finned-cylinder is better than that of the space-plane. Indeed, the finned-cylinder generates resultant aerodynamic force higher than that of the space-plane (see Fig. 4(d)). Furthermore, longitudinal equilibrium ($C_{MzCG}=0$) at $\alpha=0$ deg is stable ($dC_{MzCG}/d\alpha < 0$). On the contrary, equilibrium for the space-plane is unstable ($dC_{MzCG}/d\alpha > 0$). Table 7 reports the values of the stability derivatives for the space-plane and of the finned-cylinder at the three altitudes. The comparison of the aerodynamic behavior of the finned-cylinder with both Orion and the space-plane in terms of global aerodynamic coefficients indicates that the finned-cylinder would be better.

Table 8 Relative increases of heat flux and wall temperature at the stagnation point with respect to those of Orion

h [km]	Finned-cylinder		Space-plane	
	$\Delta\dot{q}(0)/\dot{q}(0)$	$\Delta T_w(0)/T_w(0)$	$\Delta\dot{q}(0)/\dot{q}(0)$	$\Delta T_w(0)/T_w(0)$
100	0.20	0.05	0.34	0.08
90	0.70	0.14	1.12	0.21
80	2.65	0.40	5.52	0.60
70	2.19	0.43	11.82	0.98
60	0.86	0.12	12.37	0.91

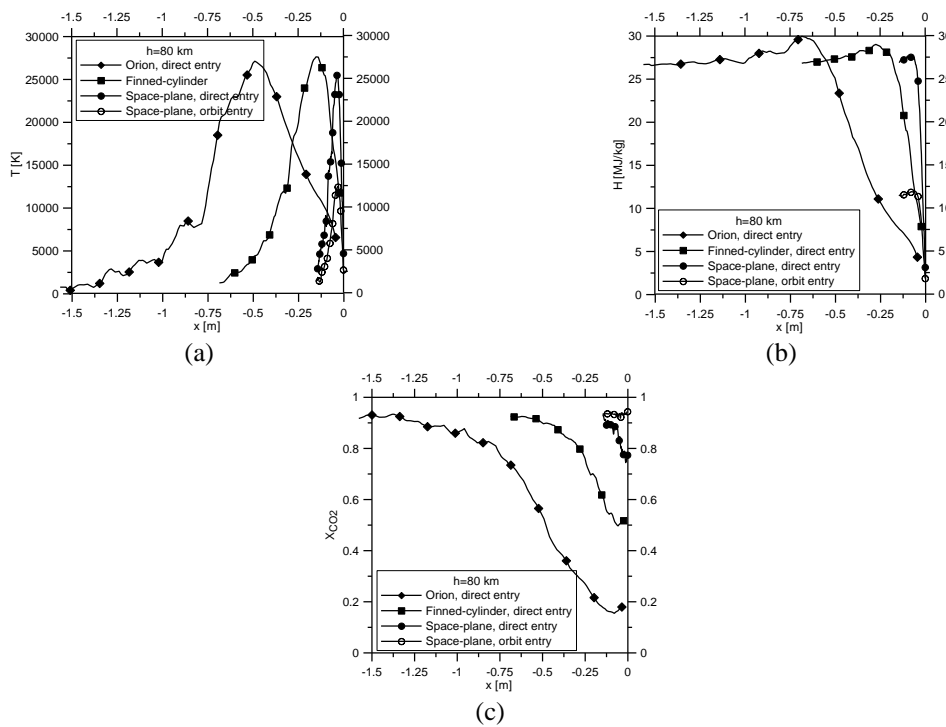


Fig. 6 Profiles of temperature (a), flow total enthalpy (b) and molar fraction of CO₂ (c) along the stagnation line: h=80 km

Figs. 5(a), 5(b) and 5(c) show the profiles of heat flux, wall temperature and pressure at the stagnation point as functions of altitude. It seems that the behavior of Orion is better from a thermal point of view than those of finned-cylinder and of space-plane. Heat flux and wall temperature for Orion are lower than those of the finned cylinder and of the space-plane because characterized by a larger curvature radius at the stagnation point (R_s): $R_s=6.04$ m for Orion (Zuppardi 2020), 0.8 m for finned-cylinder (Zuppardi and Mongelluzzo 2021a, b), 0.0416 m for the space-plane. According to Zoby (1968), the heat flux is linked to the inverse of square root of R_s by:

$$\dot{q}(0) = K \sqrt{\frac{p(0)}{R_s}} (H - h_w) \tag{2}$$

being: K a constant, $p(0)$ the pressure at the stagnation point in atmospheres, H the flow total enthalpy ($H=c_p T+V^2/2$), h_w the thermodynamic enthalpy at wall conditions ($h_w=c_p T_w$). Table 8 reports the relative increases of heat flux and surface temperature at the stagnation point of the finned-cylinder and of the space-plane with respect to those of Orion.

Figs.6(a), 6(b) and 6(c) show the influence of the shape of the Orion heat shield, the finned-cylinder ogive and the space-plane nose on the profiles of temperature (a), total flow enthalpy (b), carbon dioxide molar fraction (c) along the stagnation line, for example, at $h=80$ km. Indeed, the different body shapes produce shock waves of different thickness. As expected, being the curvature radius of the finned-cylinder intermediate between Orion and space-plane also the corresponding profiles are intermediate. The smaller the curvature of the body, the softer the profile of each aero-thermo-dynamic quantity and therefore of the corresponding gradient. Furthermore, for the nose of the space-plane the aerodynamic quantities are in line with what one could expect from the two entry trajectories.

8. Conclusions

According to the NASA Artemis program, Orion has been designed besides as a rescue shuttle for the ISS, also for the transportation of instruments and astronauts to Moon, Mars and beyond. For this reason, Zuppardi computed the global aerodynamic coefficients of Orion along a high altitude entry path in Mars atmosphere. Zuppardi and Mongelluzzo also proposed, as a viable alternative to Orion, a blunt cylinder provided with flapped fins. Computations verified that Orion is better than the finned-cylinder to produce an aerodynamic force at low angles of attack for slowing down the capsule. On the contrary, the finned-cylinder is better in terms of attitude control capability.

The purpose of the present paper has been comparing Aerodynamics of Orion and of the finned-cylinder with that of a hypothetical, winged space-plane, similar in shape and dimensions to the Italian Flight Test Bed (FTB_2), in high altitude Mars entry path. The analysis relied on three codes: 1) a home made code, for the computation of entry trajectory; both direct and orbit entry trajectories were considered, 2) DS3V solving 3D flow field and computing the global aerodynamic coefficients. Computations were carried out at the altitude of 80, 90, 100 km and in the range of angle of attack 0-40 deg, 3) DS2V solving axisymmetric flow field and computing aerodynamic and thermal stresses at the nose stagnation point. Computations were carried out at altitudes between 60-100 km.

The analysis verified that while the aerodynamic behaviour of the space-plane is comparable with that of the finned-cylinder, the aerodynamic and thermal stresses (or pressure, temperature and heat flux) at the stagnation point are higher for the space-plane. Therefore, the finned-cylinder seems to be a valid alternative to Orion. The optimization of the geometry of the fins and of the related flaps deserves to be deepened together with an aerodynamic analysis at low altitudes or in continuum by means of computational fluid-dynamic codes.

References

- Anderson, J.D. (1998), *Hypersonic and High Temperature Gas Dynamics*, McGraw-Hill Book Company, New York, U.S.A
- Bird, G.A. (1998), *Molecular Gas Dynamics and Direct Simulation Monte Carlo*, Clarendon Press, Oxford, U.K.
- Bird, G.A. (2005), *The DS2V Program User's Guide Ver. 3.3*, G.A.B. Consulting Pty Ltd., Sydney, Australia.

- Bird, G.A. (2006a), *Visual DSMC Program for Three-Dimensional Flows, The DS3V Program User's Guide*, Ver. 2.6," G.A.B. Consulting Pty Ltd., Sydney, Australia.
- Bird, G.A. (2006b), "Sophisticated Versus Simple DSMC", *Proceedings of the 25th International Symposium on Rarefied Gas Dynamics (RGD25)*, Saint Petersburg, Russia, July.
- Bird, G.A. (2008), *Visual DSMC Program for Two-Dimensional Flows, The DS2V Program User's Guide, Ver. 4.5*, G.A.B. Consulting Pty Ltd., Sydney, Australia
- Bird, G.A., Gallis, M.A., Torczynski, J.R. and Rader, D.J. (2009), "Accuracy and efficiency of the sophisticated direct simulation Monte Carlo algorithm for simulating noncontinuum gas flows", *Phys. Fluids*, **21**(1), 017103. <https://doi.org/10.1063/1.3067865>.
- Bird, G.A. (2013), *The DSMC Method, Version 1.1*, CreateSpace Independent Publ. Platform, Charleston, South Carolina, U.S.A.
- Braun, R.D. and Manning, R.D. (2006), "Mars exploration entry, descent and landing challenges", *Proceedings of the Institute of Electrical Electronics Engineers Aerospace Conference*, Big Sky, Montana, U.S.A., March.
- Curreri, F., Guidotti, G., Russo, G., Sansone, A., Serpico, M. and Solazzo, M. (2003), "PRORA USV Program: The suborbital re-entry test", *Proceedings of the 54th International Astronautical Congress*, Bremen, Germany, September-October.
- Gallis, M.A., Torczynski, J.R., Rader, D.J. and Bird, G.A. (2009), "Convergence behavior of a new DSMC algorithm", *J. Comput. Phys.*, **28**(12), 4532-4548. <https://doi.org/10.1016/j.jcp.2009.03.021>.
- Justus, C.G. and Johnson, D.L. (2001), *Mars Global Reference Atmospheric Model 2001 (Mars-GRAM-2001) User Guide*, NASA TM 2001-210961.
- Moss, J.N. (1995), "Rarefied flows of planetary entry capsules", AGARD-R-808, 95-129, Special Course on "Capsule aerothermodynamics", Rhode-Saint-Genève, Belgium.
- Moss, J.N., Boyles, K.A. and Greene, F.A. (2006), "Orion aerodynamics for hypersonic free molecular to continuum conditions", *Proceedings of the 14th AIAA Space Planes and Hypersonic Systems and Technologies Conference*, Canberra, Australia, November.
- NASA Artemis Program (2021): <https://www.nasa.gov/specials/artemis>.
- Shen, C. (2005), *Rarefied Gas Dynamic: Fundamentals, Simulations and Micro Flows*, Springer-Verlag, Berlin, Germany.
- Roncioni, P., Ranuzzi, G., Marini, M. and Cosson, E. (2007), "Hypersonic CFD Characterization of IXV Vehicle", *Proceedings of the West-East High Speed Flow Field Conference*, Moscow, Russia, November.
- Roncioni, P., Ranuzzi, G., Marini, M., Paris, S., Cosson, E. and Walloschek, T. (2011a), "Experimental and numerical investigation of aerothermal characteristics of hypersonic intermediate experimental vehicle", *J. Spacecraft Rockets*, **48**(2), 291-302. <https://doi.org/10.2514/1.48331>.
- Roncioni, P., Ranuzzi, G., Marini, M., Battista, F. and Rufolo, G.C. (2011b), "CFD aerothermodynamic characterization of the IXV hypersonic vehicle", *Proceedings of the 7th European Symposium on Aerothermodynamics*, Brugge, Belgium, May.
- Zoby, E.V. (1968), *Empirical Stagnation-Point Heat-Transfer Relation in Several Gas Mixtures at High Enthalpy Levels*, NASA TN D-4799.
- Zuppari, G. and Savino, R. (2015), "DSMC Aero-thermo-dynamic analysis of a deployable capsule for Mars atmosphere entry", *Proceedings of the DSMC15 Workshop*, Kauai, Hawaii, U.S.A., September.
- Zuppari, G. (2020), "Aerodynamics of Orion in rarefied flow along a Mars entry path", *J. Spacecraft Rockets*, **58**(2), 531-537. <https://doi.org/10.2514/1.A34825>.
- Zuppari, G. and Mongelluzzo, G. (2021a), "Aerodynamics of a wing section along an entry path in Mars atmosphere", *Adv. Aircraft Spacecraft Sci.*, **8**(1), 53-67. <https://doi.org/10.12989/aas.2021.8.1.053>.
- Zuppari, G. and Mongelluzzo, G. (2021b), "Rarefied aerodynamics of a concept capsule alternative to Orion for Mars entry, descent, and landing", *Proceedings of the 4th International Conference on Aerospace and Aeronautical Engineering*, Valencia, Spain, October.